Available online at www.sciencedirect.com
ScienceDirect
Applied Catalysis A: General 325 (2007) 353–361
APPLIED CATALYSIS A: GENERAL
www.elsevier.com/locate/apcata

Effect of nature and surface density of oxygen species on product distribution in the oxidative dehydrogenation of propane over oxide catalysts

Evgenii V. Kondratenko [a,*], Mikhail Yu. Sinev [b,*]

[a] *Leibniz-Institut für Katalyse e.V. an der Universität Rostock, Aussenstelle Berlin, Richard-Willstätter-Str. 12, 12489 Berlin, Germany*
[b] *N.N. Semenov Institute of Chemical Physics, 4 Kosygin Street, Moscow 119991, Russia*

Received 21 July 2006; accepted 7 February 2007
Available online 3 March 2007

Abstract

Catalytic performance of non-reducible (rare-earth/alkaline-earth oxides) and reducible (vanadium-based oxides) metal oxides in auto-thermal oxidative dehydrogenation (ODH) of propane differs strongly regarding to the ratio of C_3H_6/C_2H_4. In contrast to the latter materials, ethylene is the main olefin over the former ones. In order to elucidate factors influencing the catalytic performance, a kinetic analysis of the oxidative dehydrogenation (ODH) of propane was performed. In this analysis, the ODH reaction is assumed to occur via formation and further transformations of free propyl radicals. It was demonstrated that the overall reaction rate of these both processes is affected by both strength and density (surface concentration) of oxidising active sites. However, the ratio of propene-to-ethylene is mostly affected by the density of oxidising sites (DOS), and to much less extent by their strength. High DOS is essential for further ODH of propyl radicals to propene and, therefore, for suppression of concurrent cracking reaction channel yielding ethylene.

Keywords: Oxidative dehydrogenation of propane; Oxygen adsorption; Reaction mechanism; Kinetic modelling; Temporal analysis of products (TAP) reactor; Mechanism; Vanadia

1. Introduction

Oxidative dehydrogenation (ODH) of light alkanes attracts not only scientific but also industrial attention, since it may open a potentially efficient way to produce olefins from relatively cheap and abundant feedstocks. However, this reaction suffers from low olefine selectivity at high alkane conversions. The accessible yields of desired product in oxidative conversion of light alkanes are determined by kinetic factors, i.e. overall reaction network and kinetic parameters of ''elementary'' reactions. Therefore, deep fundamental understanding of catalytic reactions at near to elementary reaction step level is of prime importance for catalyst development. The potential of the most of commonly used spectroscopic techniques applied for mechanistic and kinetic investigations of the ODH reactions is, however, very limited due to the fact that they proceed at relatively high temperatures and the concentrations of surface and gas intermediates are usually very low. This is why the thorough kinetic analysis is among of a few tools, which can be used for mechanistic studies of these processes. Besides, transient experiments in the temporal analysis of products (TAP) reactor are also very useful for deriving mechanistic insights into individual reaction steps at near to elementary level.

Based on the above backgrounds, steady-state ambient pressure catalytic tests, microkinetic simulations and mechanistic investigations in the TAP reactor were applied for studying the reaction network of the propane ODH reaction over two families of catalysts, i.e. materials based on non-reducible (rare-earth/alkaline-earth metal) and reducible (vanadia) oxides. The work was aimed at further elucidation of factors determining catalytic performance in the propane ODH reaction and at elaboration of approach of rational catalyst design. Special attention has been paid to the competition between ODH and cracking reactions, with the latter leading to the formation of

* Corresponding authors. Tel.: +49 30 63924448; fax: +49 30 63924454.
E-mail addresses: evgenii.Kondratenko@catalysis.de, evgenii@aca-berlin.de (E.V. Kondratenko), mysinev@rambler.ru (M.Yu. Sinev).

0926-860X/$ – see front matter © 2007 Elsevier B.V. All rights reserved.
doi:10.1016/j.apcata.2007.02.041

ethylene. Oxidative dehydrogenation of propane (ODP) was chosen as a model reaction to study the influence of catalyst surface chemistry and homogeneous gas-phase processes on reaction pathways and product distribution. In this work propene-to-ethylene ratio is used as such a criterion during the modelling of the ODP reaction. The catalysts were chosen taking into account the fact they differ in their ability for generation of active surface oxygen species from gas-phase O_2. It is well known, that this catalyst property influences catalytic performance [1].

2. Experimental

2.1. Catalysts

V_2O_5 (Merck), γ-Al_2O_3 (Degussa) and boehmite (Disperal, Condea) were used for catalyst preparation. The required amount of V_2O_5 was dissolved in oxalic acid at 348 K followed by adding 1 g of polyvinyl alcohol (PVA) under stirring until the solution became clear; then the same amount of boehmite and γ-Al_2O_3 (2 or 4 g) were added to the solution under continuous stirring. From the resulting mixture water was evaporated at 333 K for 12 h followed by calcination at 973 K for 6 h in air. In the present study, a sample with V loading of 4.6 wt% (designated as VO_x(4.6 wt%)/γ-Al_2O_3) was used. Details on catalyst characterization by BET, EPR, XRD, electrical conductivity, and *in situ* UV/Vis-DRS spectroscopy as well as H_2-TPR have been described elsewhere [2].

2.2. Catalytic tests in continuous-flow regime

Catalytic measurements were performed at ambient pressure under isothermal and auto-thermal conditions using two different reactors and heating devices. The isothermal tests were carried out in a U-type fixed-bed reactor made of quartz (i.d. = 6 mm). The quartz reactor was immersed into a fluidized bed of sand serving as a source of heat or its removal. Catalyst was diluted with similarly sized quartz particles for further temperature control. Catalyst particle size was between 255 and 350 μm. The feed consisted of 15 vol% oxygen and 30 vol% propane in nitrogen; the latter gas was used as internal standard for gas chromatographic product analysis (HP-5890 equipped with Poraplot Q and Molsiev 5 columns).

The oxidative conversion of propane under auto-thermal conditions was studied at atmospheric pressure in a continuous-flow tubular fixed-bed reactor ($Ø_{in}$ = 5 mm) using a $C_3H_8/O_2/N_2$ = 40/20/40 reaction mixture. The reactor along with heating and insulating arrangements has been described previously [3]. The reactor was packed with 0.2 g of catalyst without dilution with quartz particles. The total gas flow was fixed to 200 ml (STP)/min. Temperature profile inside the catalyst bed was measured by a movable thermocouple located axially in the catalyst bed.

2.3. Transient catalyst tests

Transient studies were performed in the temporal analysis of products (TAP-2) reactor, which has been comprehensively described elsewhere [4]. The catalyst (sieve fraction 250–350 μm) was packed in the micro-reactor made of quartz (40 mm length and 6 mm i.d.) between two layers of quartz of the same particle size. The catalyst amount was fixed to 50 mg. Before each experiment the catalyst was treated in a flow of O_2 (30 ml/min) at 873 K and ambient pressure for ca. 1 h. Hereafter, the micro-reactor was evacuated to 10^{-5} Pa and the reactor temperature was set to the desired values (573–823 K). Pulses containing small amounts of reactants (10^{14} to 5×10^{14} molecules per pulse) diluted by an inert gas were injected into the micro-reactor. For such pulse sizes, gas transport through the reactor is in the Knudsen diffusion regime. This means that the transient responses are a function of gas–solid interactions and not influenced by collisions between gas-phase molecules. Thus, heterogeneous reaction steps are under investigation. C_3H_8/O_2 as well as single O_2 and C_3H_8 interactions with the VO_x(4.6 wt%)/γ-Al_2O_3 catalyst were studied using the following reaction mixtures: $C_3H_8/^{18}O_2$/Ne = 2/1/2, O_2/Ne = 1/1 and C_3H_8/1 = 1/1.

The feed components, reaction products and inert gas were monitored at respective atomic mass units (AMUs) using a quadruple mass spectrometer (HAL RC 301 Hiden Analytical). The following AMUs were used for identification of the various compounds: 132 (Xe), 48 ($C^{18}O_2$), 46 ($C^{18}O^{16}O$), 44 ($C^{16}O_2$ and C_3H_8), 42 (C_3H_8 and C_3H_6), 36 ($^{18}O_2$), 34 ($^{18}O^{16}O$), 32 ($^{16}O_2$), 30 (C_2H_6), 29 (C_3H_8), 28 (C_3H_8, C_3H_6, $C^{16}O$ and $C^{16}O_2$), 25 (C_2H_4), 20 (Ne), 18 (H_2O), 15 (CH_4). The concentrations of feed components and reaction products were determined from the respective AMUs using standard fragmentation patterns and sensitivity factors. For each AMU pulses were repeated 10 times and averaged to improve the signal to noise ratio. In the experiments, Ne (99.995), Xe (99.99), O_2 (99.995), $^{18}O_2$ (98% ^{18}O atoms), C_3H_8 (99.95), were used. The $^{18}O_2$ oxygen isotope was purchased from ISOTEC.

2.4. Kinetic model and evaluation procedure

2.4.1. Treatment of data from transient experiments

The parameter estimation procedure based on a numerical solution of partial differential equations, which describe the processes of diffusional transport, adsorption/desorption and the catalytic reaction inside the TAP reactor, was reported earlier [5,6]. The used software code allowed the implementation of different kinetic models.

2.4.2. Kinetic model for – irreversible dissociative adsorption of O_2

Irreversible dissociative adsorption of oxygen occurs on two catalytically active sites. The model was chosen based on experimental data on oxygen isotopic exchange [7] and modelling the oxidative dehydrogenation of propane [8] over vanadium-based catalysts. The mechanistic model and the oxygen-mass balances for data evaluation can be written as follows:

- oxygen adsorption on catalyst surface sites denoted as z

$$O_2 + 2z \xrightarrow{k_{ads}} 2z{-}O \quad (1)$$

mass balance of gas-phase oxygen

$$\frac{\partial C_{O_2}}{\partial t} = D_{eff}\frac{\partial^2 C_{O_2}}{\partial x^2} - k_{ads}C_{tot}^2(1-\Theta_O)^2 C_{O_2} \quad (2)$$

mass balance of surface species

$$\frac{\partial \Theta_O}{\partial t} = 2k_{ads}C_{tot}C_{O_2}(1-\Theta_O)^2 \quad (3)$$

where $1 = \Theta_O + \Theta_z$, $\Theta_z = C_z/C_{tot}$, $\Theta_O = C_{z\text{-}O}/C_{tot}$ and D_{eff} the effective Knudsen diffusion coefficient.

3. Modelling of propane oxidation

The main principles and procedures of modelling the kinetics of LA (light alkane) oxidative transformations are discussed in detail elsewhere [9,10]. Here we have to mention, that the processes under consideration with high probability proceed via the formation and further transformations of free radicals (FR) [11–13]. This means that multiple reactions of FR – both homogeneous and heterogeneous – should be taken into account in the kinetic model. As a result, the overall process can be represented by a kinetic scheme that includes homogeneous and heterogeneous elementary reactions of initial reactants (alkane, oxidant), reactive intermediates such as FR and molecular products including target products of partial oxidation, e.g. olefins and/or oxygenates. The values of kinetic parameters for homogeneous reactions are available in the corresponding literature, including review articles and databases (see, for instance [14–18]). Concerning the heterogeneous reaction pathways, it was earlier demonstrated [19,20] that the main types of heterogeneous transformations (H-atom transfer, O-atom transfer, radical capture) can be described in the same terms as elementary reactions in the gas phase, and their activation energy can be evaluated using the thermochemical information obtained from independent calorimetric experiments (see Table 1).

The above approach was used in the present work. A set of elementary homogeneous reactions was compiled according to the principles discussed in [9,10]. Reactions of gas-phase and surface species containing one to three carbon atoms have been considered. The ''homogeneous'' reaction network was supplemented with a set of heterogeneous reactions, which includes reactions of propane, propene, and ethylene, as well as reactions of *n*- and *iso*-propyl radicals. Multiple reactions of O-containing C_3-species were ignored. Of course, this substantially lowered the predictive power of the model. However, since in the framework of this study we were mostly interested in the propene-to-ethylene ratio in the reaction mixture, this simplification can be considered as acceptable.

The set of heterogeneous processes treated in the framework of the model includes the reactions of surface active sites in three different states:

- $[O]_S$: oxidised sites, which are active for H-atom abstraction from any species;
- $[OH]_S$: hydroxylated sites, which arise from the reaction of $[O]_S$ site with any H-containing species;
- $[\ ]_S$: reduced sites, i.e. oxygen vacancy forming during dehydroxylation or in the course of $[O]_S$ reaction with species possessing high O-atom affinity (e.g., CO molecule, CH_3 radical, etc.).

A particular chemical nature of the above forms of active sites depends on the composition of the catalyst under consideration. In this work we have focused mainly on the reaction kinetics in the presence of a V-containing catalyst, which is efficient in the formation of propene during propane oxidation. In this case the $[O]_S$ sites can be equated to vanadyl V^{5+}=O and/or bridge V^{5+}–O–M (where M—metal cation in the next cationic position; it can be V atom or metal atom from catalyst support or modifying additive) species. Hydrogen abstraction from gaseous species leads in these cases to the

Table 1
Main types of heterogeneous elementary reactions of radicals accounted in the model (according to [19–21])

Reaction types	Parameters of Polanyi–Semenov equation[a]		Examples
	a	*b*	
H-atom transfer	40 (endothermic) 40 (exothermic) 0[b] (both endo- and exothermic)	1 (endothermic) 0.2 (exothermic) 1[b] (endothermic) 0[b] (exothermic)	$[O]_S + CH_4 \rightarrow [OH]_S + CH_3$ $[O]_S + H_2O_2 \rightarrow [OH]_S + HO_2$ $[OH]_S + CH_3 \rightarrow [O]_S + CH_4$ $[O]_S + C_2H_5 \rightarrow [OH]_S + C_2H_4$ $[OH]_S + HO_2 \rightarrow [O]_S + H_2O_2$ $[OH]_S + O_2 \rightarrow [O]_S + HO_2$
O-atom transfer	0 (both endo- and exothermic)	1 (endothermic) 0 (exothermic)	$[\ ]_S + HO_2 \rightarrow [O]_S + OH$ $[O]_S + H \rightarrow [\ ]_S + OH$ $[O]_S + CH_3 \rightarrow [\ ]_S + CH_3O$ $[\ ]_S + CH_3O \rightarrow [O]_S + CH_3$ $[O]_S + CO \rightarrow [\ ]_S + CH_3O$
Capture	0	0	$[\ ]_S + C_2H_5O \rightarrow [OC_2H_5]_S$ $[O]_S + H \rightarrow [OH]_S$
Decomposition	40	1	$[OC_2H_5]_S \rightarrow [OH]_S + C_2H_4$

[a] In the form $E_a = a + b\Delta H$.
[b] If transferred between two O-atoms.

formation of terminal or bridge OH-groups bound to V^{4+} cations, whereas anion vacancy $[\ ]_S$ sites can be associated with reduced V^{3+} sites.

Heterogeneous processes, which proceed during the catalyst re-oxidation via two routes (via dehydroxylation (Eq. (4))) and via reaction of $[OH]_S$ sites with gas species (O_2 molecules, RO, RO_2 radicals, etc.) according to Eq. (5), have been considered in detail elsewhere [21]. In this work it was assumed that the dehydroxylation of V-containing catalyst could proceed with relatively low activation energy (22 kcal/mol). Concerning the second re-oxidation route, i.e., direct reaction of $[OH]_S$ with gas-phase species X (Eq. (5)), we just mention here that, according to the accepted approach [19], activation energies of each elementary step is determined by the enthalpy change. The latter in its turn is strongly dependent on the $E_{O–H}$ value (Eq. (6)).

$$2V^{4+}{-}OH \rightarrow V^{5+}{=}O + V^{3+}{-}[\,] + H_2O \quad (4)$$

$$[OH]_S + X \rightarrow [O]_S + XH \quad (5)$$

$$\Delta H = E_{O–H} - E_{X–H} \quad (6)$$

In other words, since both reduction and re-oxidation of active sites are dependent on the $E_{O–H}$ value, their rates are correlated: the faster the reduction, the slower the re-oxidation via dehydrogenation route at a given temperature and equal other conditions.

In addition to the steps discussed earlier [19–21], it was assumed that V^{3+}–[ ] sites can undergo a fast direct re-oxidation by H_2O_2 molecules according to the following equation:

$$V^{3+}{-}[\,] + H_2O_2 \rightarrow V^{5+}{=}O + H_2O \quad (7)$$

Kinetic simulations have been performed for a well-stirred quasi-homogeneous reaction system (active catalytic sites are uniformly distributed in the reacting gas) in isothermal regime at 773 K, at atmospheric pressure and initial $C_3H_8/O_2/N_2$ = 2/1/4 gas composition. In most cases concentration of active catalytic sites was calculated taking into account the density and the specific surface area of V-alumina catalyst equal to 0.8 g/ml and 48 m^2/g, respectively.

The strength and the concentration (''surface density'') of O-containing active sites have been treated as variables during the modelling. H-atom affinity of active site (O–H binding energy) is considered as the measure of the strength of the active site and varied for V-containing catalyst from 50 to 75 kcal/mol. Surface density of oxidising sites (DOS) was varied from 1×10^{13} to 1×10^{16} sites/m^2. These DOS values correspond to $\sim 3 \times 10^{-5}$ and $\sim 3 \times 10^{-2}$% of total number of surface sites, respectively.

It should be emphasised here that at higher DOS values the total number of active sites in the unit volume of the reaction space becomes comparable with the concentration of reacting particles in the gas phase. For instance, at 773 K and 1 bar the total number of species in 1 cm^3 is ca. 10^{19}. For the catalyst with a bulk density of ca. 0.8 g/cm^3 and specific surface area of 48 m^2/g (similar to the V-containing catalyst used in this work) the total number of surface sites in 1 cm^3 exceeds 5×10^{20} (if a lattice parameter is about 2×10^{-10} Å). These numbers indicate that the DOS value corresponding to 0.1% of the total number of surface sites on the other hand corresponds to the volume concentration in the reaction space close to oxygen concentration in air at 773 K and atmospheric pressure. This creates some difficulties for simulations associated with uncertainty in the steady-state distribution of the above forms of active sites, i.e. $[O]_S$, $[OH]_S$ and $[\ ]_S$. In real experiments such distribution is reached after some transition period, during which the total amount of reactants has passed through the catalyst layer, can by far exceed the number of active sites. However, in the calculations performed for non-flow reactor, the total number of species of each type is fixed from the beginning. This means that not only oxygen and hydrocarbon concentrations, but also the initial (at zero time) distribution of active sites determine the amount of oxidant and reductant in the mixture. In such a case the active sites cannot be longer considered as ''catalytic'', but they contribute to the composition of the final mixture. This is a serious limitation, which does not allow performing simulations with high DOS values. The latter can be achieved, however, in real catalytic systems, first of all in those containing redox cations such as V, Mo, W.

4. Results

4.1. Continuous-flow catalytic tests at ambient pressure

The propane ODH reaction over VO_x(4.6 wt%)/γ-Al_2O_3 was performed both under isothermal and auto-thermal conditions. The steady-state performance under isothermal conditions has been reported previously [2]. C_3H_6, CO and CO_2 were the main gas-phase carbon-containing reaction products. It was established that the CO_x products originate manly via consecutive propene oxidation. Propene is a primary product of the propane ODH reaction. In the present study, a C_3H_8/O_2 ($C_3H_8/O_2/N_2$ = 40/20/40) reaction mixture was ignited above a certain reaction temperature producing enhanced heat generation. This reaction heat resulted in an increase of temperature in the catalyst bed up to ca. 1200 K. The catalytic reaction further proceeded without external heating (auto-thermally). Similar phenomena have been repeatedly reported for Pt-based catalysts [22–26] and catalytic materials consisting of rare-earth or alkali-earth metal oxides [22,27]. In agreement with the isothermal performance of VO_x(4.6 wt%)/γ-Al_2O_3, C_3H_6, CO and CO_2 were also observed as the main reaction products. C_2H_4 was identified in low amounts only. However, this observation disagree with the results previously reported for catalytic materials based on rare-earth metal oxides and noble metals [22–26]. Over the latter materials, not propene but ethylene was the predominant olefin in the course of auto-thermal propane oxidation. Table 2 compares the ratio of C_3H_6/C_2H_4 over various catalytic materials. This ratio is in the range of 0.6–1.2 over Pt-containing catalysts and rare-earth metal oxides. In contrast to these catalytic systems, this ratio over the VO_x(4.6 wt%)/γ-Al_2O_3 catalyst is ca. 25. It is worth noticing that the difference in the propene-to-ethylene ratio between these two types of catalysts cannot be exclusively explained by

Table 2
Catalytic performance of various catalytic materials in the ODP reaction ($X(O_2)$ = 100%, C_3H_8/O_2 = 66.6/33.3[a], $C_3H_8/O_2/N_2$ = 56.6/23.3/20[b], $C_3H_8/O_2/N_2$ = 40/20/40[c])

Catalysts	$T_{furnace}$ (K)	T_{max} (K)	$X(C_3H_8)$ (%)	$Y(C_3H_6)$ (%)	$Y(C_3H_6)/Y(C_2H_4)$	Ref.
Pt(5 wt%)/γ-Al_2O_3[a]		1145	64	12.2	0.9	[24]
Pt-10%Rh 80 mesh[b]	923		45	15.6	1.25	[23]
$SmNa_{0.0028}P_{0.0014}O_x$[c]	539	833	30.5	5.8	0.63	[27]
VO_x(4.6%)/γ-Al_2O_3[c]	623	931	23	11.3	24.6	Present

thermal (non-catalytic) cracking of C_3 hydrocarbons, since the reaction temperature in the catalyst bed was very similar for all the catalysts in Table 2. Therefore, the observed product distribution should be related to catalytic (or catalyst-assisted) reactions. For identifying the properties of the catalysts, which determine their ability to ignite a C_3H_8/O_2 mixture and to produce olefins under conditions of auto-thermal propane oxidation, mechanistic studies of this reaction were performed in the TAP reactor. These experiments are excellently suitable for mechanistic analysis of short contact time alkane dehydrogenation due to the following reasons: (i) TAP experiments are performed at millisecond contact times; (ii) isothermal conditions are ensured; (iii) gas-phase reactions are minimized as compared to heterogeneous ones. The results are presented and discussed in the next section.

4.2. TAP results

4.2.1. Sequence of product formation upon C_3H_8 oxidation over VO_x species in the absence of gas-phase O_2

The effect of lattice oxygen or adsorbed oxygen species on propane oxidation over VO_x(4.6 wt%)/γ-Al_2O_3 was studied by means of C_3H_8 (oxygen-free conditions) and of $^{18}O_2$–C_3H_8 pulse experiments. In the former case, C_3H_6, CO, and CO_2 were observed as main carbon-containing reaction products. No measurable amounts of C_2H_4 were detected. However, C_2H_4 has been previously observed, when propane was pulsed over rare-earth metal oxides having been pre-treated by O_2 pulses [27]. The difference between VO_x(4.6 wt%)/γ-Al_2O_3 and rare-earth metal oxides in ethylene formation from propane under transient vacuum conditions is in a good correspondence with the results of steady-state catalytic tests at atmospheric pressure (Table 2).

Since gas-phase oxygen was not present in the C_3H_8 pulse, all the reaction products were formed by C_3H_8 and/or C_3H_6 oxidation at the expense of lattice oxygen of VO_x species. Propene transient response was observed immediately after propane, whereas the responses of formaldehyde and CO_x are delayed. Formaldehyde was identified by using isotopically labeled VO_x species ($V^{18}O_x$). The order of appearance of the reaction products in Fig. 1 can be interpreted as follows. Since the transient response of C_3H_6 appears immediately after C_3H_8 and its transient response is slightly narrow than that of C_3H_8, it is concluded that C_3H_6 is directly formed from C_3H_8 via oxidative dehydrogenation. The primarily formed propene reacts further at the C–C bond yielding formaldehyde followed by its further oxidation to CO and CO_2. The secondary nature of CO_x formation (consecutive propene oxidation) agrees with the previously reported steady-state selectivity–conversion relationship at ambient pressure [2].

4.2.2. Active oxygen species

In order to elucidate the role of different oxygen species in propane oxidation under transient vacuum conditions, a mixture of propane with labelled ($^{18}O_2$) oxygen was pulsed over the VO_x(4.6 wt%)/γ-Al_2O_3 catalyst. The product spectrum in this experiment did not change from the one obtained when propane reacted with the catalyst in the absence of gas-phase oxygen. Besides, no ^{18}O insertion into CO_x molecules was observed. Based on the latter fact it is concluded that only lattice oxygen from VO_x takes part in the formation of CO_x in the conditions applied. It is generally accepted [28] that the transformation of gaseous oxygen into the form of lattice anions proceeds via several intermediate states of different lifetime and reactivity (e.g. various di- and mono-atomic forms of oxygen differently oriented in the coordination sphere of V ion and carrying different charges). Nevertheless, in the case of propane oxidation over V-alumina catalyst only the final state, which can be considered as ''lattice'' oxygen, contributes to the activation of propane molecule and the formation of final products. In our TAP experiments, labelled gas-phase $^{18}O_2$ was only consumed for catalyst regeneration; i.e. it was dissolved in a very large reservoir of lattice ^{16}O oxygen. Due to a low degree of catalyst reduction in each pulse, re-oxidation step becomes kinetically irrelevant. Unlike this, in the steady-state catalysis at atmospheric pressure, the mechanism and the kinetics of re-oxidation or reduced VO_x species can become crucial for the

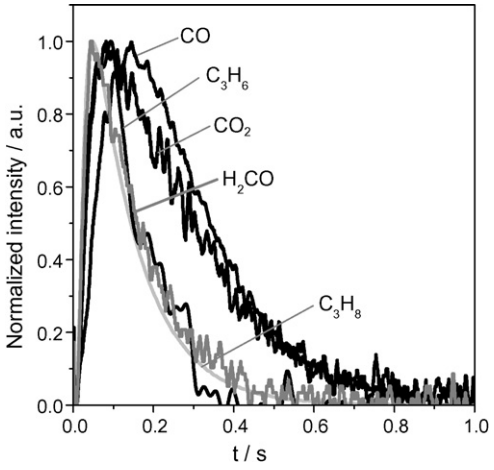

Fig. 1. Transient responses upon C_3H_8 (C_3H_8/Ne = 1/1) pulsing over VO_x(4.6%)/γ-Al_2O_3 at 823 K. Pulse size of C_3H_8 is ca. 5×10^{14} molecules.

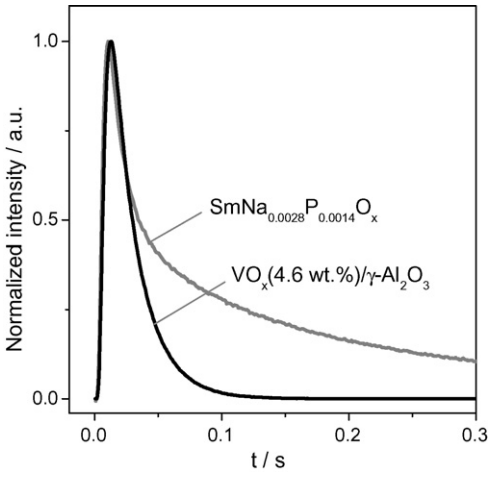

Fig. 2. Normalized transient responses of oxygen when pulsing an O_2–Ne (O_2/Ne = 1/1) mixture over different catalysts at 823 K. Pulse size of O_2 is ca. 10^{14} molecules.

overall process and may cause the difference in catalytic behaviour of different materials.

Fig. 2 illustrates oxygen transient responses over VO_x(4.6 wt%)/γ-Al_2O_3 and $SmNa_{0.0028}P_{0.0014}O_x$, when O_2 was pulsed over the catalysts at 773 K. The responses are normalized for better comparing of their shapes, since they reveal important mechanistic and kinetic information on chemical and transport phenomena inside the reactor. It is clearly that the transient responses in Fig. 2 differ strongly in their shapes. This observation indicates that gas-phase oxygen differently reacts with VO_x(4.6 wt%)/γ-Al_2O_3 and $SmNa_{0.0028}P_{0.0014}O_x$ catalytic materials. As reported in our previous work [29], O_2 adsorbs reversibly and dissociatively over $SmNa_{0.0028}P_{0.0014}O_x$ via a molecular surface precursor. For deriving mechanistic insights into O_2 interaction with VO_x(4.6 wt%)/γ-Al_2O_3, the respective oxygen transient response was fitted to the kinetic model described in Section 2.4. A comparison of experimental oxygen response and the simulated one is presented in Fig. 3. It is obvious that the model describes the experimental data very well. This observation is in agreement with experimental data on isotopic exchange of oxygen [5] and kinetic modelling of ODP [7] and O_2 adsorption [30] over vanadium-based catalytic materials. Taking into account the results of ambient pressure catalytic experiments in Table 2 as well as of transient experiments with C_3H_8 and O_2 in Figs. 1 and 2, the difference in propane ODH performance of reducible and non-reducible metal oxides may be related to the nature of oxygen species or to their surface coverage. These aspects are discussed in Section 5 together with the results from Section 4.3.

4.3. Modelling

4.3.1. Reaction rate and $C_3^=/C_2^=$ ratio: effect of DOS and $E_{O–H}$

As mentioned in Section 3, the procedure accepted for modelling does not allow running simulations using high (close to realistic) DOS values due to a strong uncertainty in the steady-state concentration of the catalyst active sites. Nevertheless, the results obtained at varied DOS and strength of active sites ($E_{O–H}$) have provided additional important mechanistic information. All results presented in this section were obtained assuming that at $t = 0$ all active sites are in an intermediately reduced, i.e. $[OH]_S$ state.

The effect of DOS was studied for the constant $E_{O–H}$ = 74.5 kcal/mol. As can be seen in Fig. 4, at low DOS ($\leq 1 \times 10^{13}$ sites/m^2, which corresponds to the fraction of the total number of surface sites $\sim 10^{-7}$ to 10^{-6}), the shape of ''rate versus conversion (time)'' curve(s) is typical for self-accelerating homogeneous chain reactions. As the DOS values exceeds 1×10^{15} sites/m^2, or 10^{-2}% of the total number of surface sites, the process becomes more ''linear'', i.e. it starts with the maximum rate, which decreases as the concentration of reactants becomes lower.

Relative amounts of olefins ($C_3^=/C_2^=$ ratio) in the reaction mixture strongly depends on the DOS value: whereas at low DOS the amount of two olefins are comparable, at high DOS the amount of ethylene becomes almost negligible, especially at relatively high conversions. Upon increasing propane conversion, the $C_3^=/C_2^=$ ratio substantially increases (see Fig. 5).

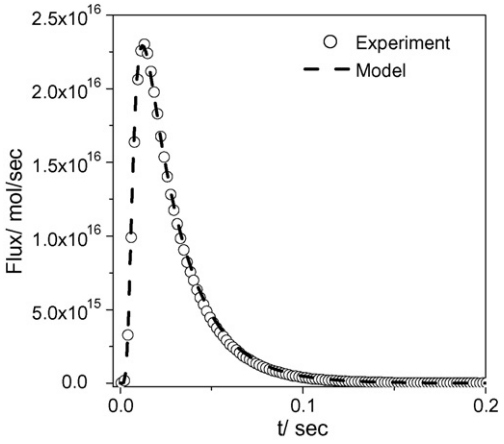

Fig. 3. Comparison between experimental and simulated responses of oxygen over VO_x(4.6%)/γ-Al_2O_3 at 823 K.

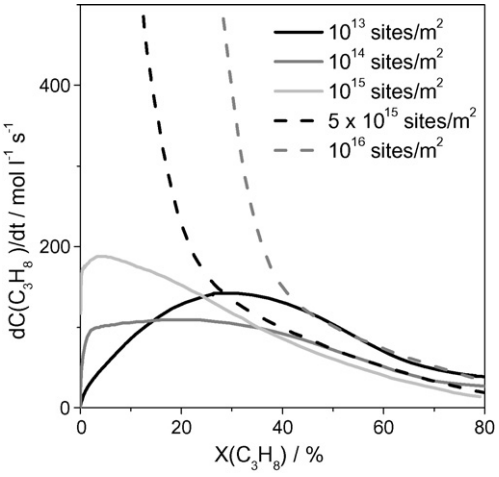

Fig. 4. Rate of reaction as a function of propane conversion at different DOS values.

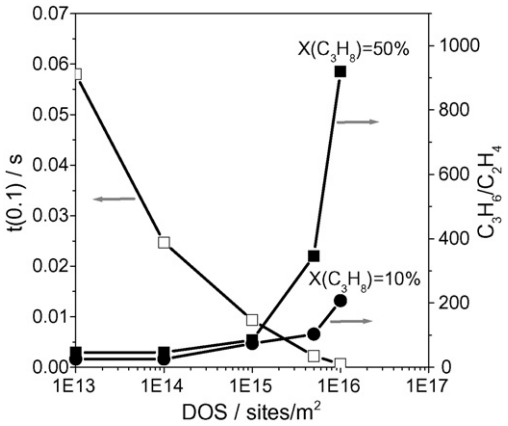

Fig. 5. Effect of DOS on the time of 10% propane conversion $t(0.1)$ and propene-to-ethylene ratio $C_3{=}/C_2{=}$ at 10% and 50% propane conversion.

The effect of the strength of the active site on catalytic performance is demonstrated in Fig. 6. These results were obtained at constant DOS (1×10^{-15} sites/m^2). From the results in Fig. 6 it is clear that the time for reaching 10% propane conversion substantially increases with an increase in O–H bond strength. This may be explained by the fact that the activation energy of the rate of catalyst re-oxidation is strongly influenced by $E_{O–H}$.

5. Discussion

The obtained experimental data demonstrate that two groups of catalysts, i.e. (i) Pt-containing, mixed rare-earth/alkaline-earth oxides and (ii) VO_x/γ-Al_2O_3, very significantly differ in their catalytic performance in the auto-thermal propane ODH reaction (Table 2). In contrast to the vanadium-based catalyst, ethylene is the main olefin over the Pt-containing catalysts and mixed rare-earth/alkaline-earth oxides. These data together with the results from Section 4.2.2 indicate that the properties of oxygen species involved into alkane molecule activation and transformations of reactive intermediates are very important for the catalytic performance. As mentioned in Section 1, the possibility of the formation of final products via free-radical intermediates has been demonstrated in several publications.

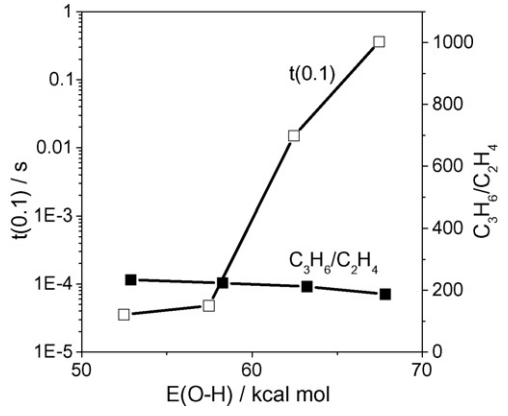

Fig. 6. Effect of strength of active site on reaction rate (time of 10% propane conversion) and olefin distribution (propene-to-ethylene ratio).

This is why in order to derive further insights into the role of the nature of oxygen species and/or their surface density, possible transformations of final and intermediate products of propane oxidation were analysed based on the model suggested previously for heterogeneous–homogeneous transformations of light alkanes [9,10]. It is demonstrated that if propyl radicals are formed as the primary intermediates, ethylene forms via cracking of propyl radicals (Eq. (8)) competing with H-atom elimination leading to propene (Eq. (9)):

$$C_3H_7 \rightarrow C_2H_4 + CH_3 \quad (8)$$

$$C_3H_7 \rightarrow C_3H_6 + H \quad (9)$$

Fig. 7 demonstrates the relative efficiency of the above reaction pathways as a function of temperature according to the existing kinetic data for the gas-phase reactions [14–18]. The ratio of the rate constants of reactions (Eq. (8)) and (Eq. (9)) determines the relative amount of two olefins formed at relatively low conversions in anaerobic conditions in the absence of catalyst (see Fig. 8). One can see that both for *iso*- and *n*-propyl radicals, propene forms predominantly and its relative amount should increase with rising temperature. Over rare-earth/alkaline-earth catalysts, however, ethylene is formed in higher concentration than propene. This can be explained by a higher reactivity of the latter in reactions of consecutive oxidation. Such reactions can proceed via the addition of various chemical groups (e.g. O-atoms) to a double C–C bond (Eq. (10)):

$$RHC{=}CH_2 + R'O_2 \rightarrow RHC\text{---}CH_2 + R'O \quad (10)$$

(with O bridging the two carbons)

In such reactions reactivities of C_3- and C_2-olefines differ not very strongly: for instance, the rate constants for reaction (10) with HO_2 radicals for propene and ethylene at 650 °C are equal to 4.5×10^8 and 1.9×10^8 cm^3 mol^{-1} s^{-1}, respectively [18]. The difference is much stronger for another type of reactions proceeding via H-atom abstraction (Eq. (11)) and

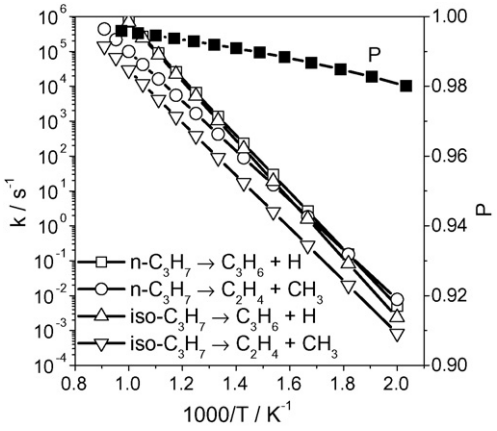

Fig. 7. Rate constants (k) of homogeneous reactions of propyl radicals and probability (P) of their heterogeneous dehydrogenation (estimated for E_a = 10 kcal/mol) vs. reciprocal temperature.

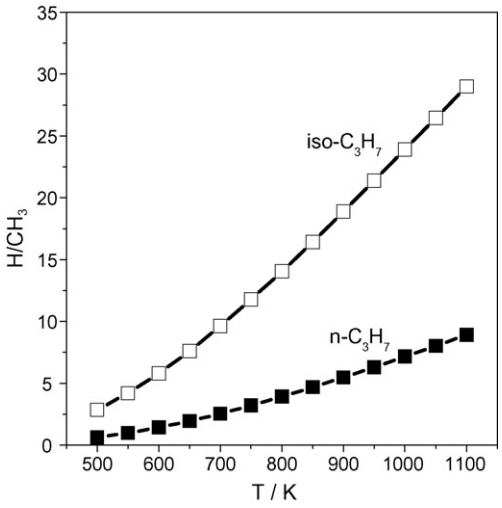

Fig. 8. Ratio of rate constants of H-atom and CH_3-radical elimination (i.e. primary $C_3{=}/C_2{=}$ formation ratio) as a function of temperature for *iso*- and *n*-propyl radicals.

further oxidation of unsaturated radicals (Eq. (12)):

$$RH + X \rightarrow XH + R \quad (11)$$

$$R + O_2 \rightarrow RO_2 \rightarrow \cdots \rightarrow CO_x \quad (12)$$

Since propene contains weakly bound allylic H-atoms in CH_3 group, its total oxidation is going to proceed much faster than that of ethylene: for instance, in the temperature range 550–650 °C the rate constant of H-abstraction from propene by O_2 molecule is ~300–700 times higher than from ethylene [18]. Although, as we mentioned above, the kinetic scheme used in this work does not fully reflect the real reaction network, it correctly explains the trends in the $C_3{=}/C_2{=}$ ratio variations with conversion.

As a rule, ODH catalysts contain active species with high affinity to H-atoms, which determine their ability to activate C–H bonds. Since the C–H bond in C_3H_7-radicals is by far less strong than in propane (~−35 versus 95 kcal/mol, respectively), H-atom abstraction from them yielding propene can proceed with very low activation energy even at very low E_{O-H} ($\leq$10 kcal/mol at $E_{O-H} > 25$ kcal/mol). In other words, at sufficiently high density of oxidising states (DOS) this reaction is much more efficient than reactions of C_3H_7-radicals in the gas phase (see Fig. 7). In this particular case, olefin distribution ($C_3{=}/C_2{=}$ ratio) is much stronger affected by DOS rather than their strength. As a result, higher DOS on V-containing catalyst(s) causes higher propene-to-ethylene ratio compared to that obtained over rare-earth oxide-based catalysts under comparable reaction conditions. We have to accentuate once again that the kinetic model used in this work to simulate product distributions is not full enough to predict the exact values of the $C_3{=}/C_2{=}$ ratio (compare the data of Table 2 and Fig. 5). However, it correctly describes the effect of the density of active sites and gives an explanation based on the difference in the energies of H-atom abstraction from parent propane molecule and propyl radicals.

The results obtained in this work demonstrate that the propane ODH reaction rate is controlled by re-oxidation of reduced sites over V-containing catalysts. This conclusion is consistent with the data obtained earlier (see, for instance [31,32]), which indicate that the oxidation degree of vanadium in supported V-alumina catalysts under steady-state conditions can be as low as V^{3+} at high degrees of propane conversion (near to complete oxygen conversion), when optimum yields of ODH products can be achieved. Moreover, the additives capable of accelerating the re-oxidation process (e.g., antimony) also strongly improve the overall catalytic performance in ODH of light alkanes.

Our TAP results demonstrate that lattice oxygen of V-alumina catalyst is involved into the formation of carbon oxides in the course of propane oxidation. This is in a good agreement with the data obtained earlier using the *in situ* differential scanning calorimetry (DSC) [32]: although the reduction of V-alumina catalysts by light alkanes leads to a progressive increase of lattice oxygen binding energy and somewhat decrease of its reactivity, the formation of total oxidation products proceeds in parallel with ODH. According to [32], the ODH process at the expense of lattice oxygen stops when the average oxidation degree of vanadium in the catalyst reaches the V^{3+} state. After that the formation of olefin continues in non-oxidative mode, i.e. molecular hydrogen forms as the second product.

According to the TAP data, the characteristic time of the formation of carbon oxides is much longer than for propene formation (see Fig. 1). They keep forming even when the parent propane pulse is left the catalyst bed. This is a strong evidence for the existence of the heterogeneous pathway of total oxidation, likely due to the formation (Eq. (13)) and consecutive transformations (Eq. (14)) of adsorbed species such as alkoxides:

$$[O]_S + C_3H_7 \rightarrow [OC_3H_7]_S \quad (13)$$

$$[OC_3H_7]_S + n[O]_S \rightarrow 3CO_x + 3H_2O + [OH]_S + n[\,]_S \quad (14)$$

Since reaction (14) requires the participation of several (from six to nine) lattice oxygen atoms, its rate is controlled by a diffusion flow and progressively decreases with increasing degree of reduction. The latter results in the increasing ODH selectivity.

6. Conclusions

The analysis of reaction network of propane oxidation over reducible and non-reducible metal oxide catalysts using catalytic tests under steady-state and transient conditions accompanied by kinetic modelling demonstrates that selectivity of propene formation is affected by the nature and the density of oxidising states (DOS). High DOS is essential for further ODH of propyl radicals and, therefore, suppression of concurrent cracking reaction channel. This knowledge may eventually be used for further improvement of catalytic materials and process operation.

Acknowledgements

Support by Deutsche Forschungsgemeinschaft (DFG) within the frame of the competence network (Sonderforschungsbereich 546) ‘‘Structure, dynamics and reactivity of transition metal oxide aggregates’’ and by AURUS Marketing Services GmbH (Vienna, Austria) has been greatly appreciated.

References

[1] O.V. Buyevskaya, M. Baerns, Catalysis 16 (2002) 155.
[2] E.V. Kondratenko, M. Baerns, Appl. Catal. A 222 (2001) 133.
[3] S.A.R. Mulla, O.V. Buyevskaya, M. Baerns, J. Catal. 197 (2001) 43.
[4] J.T. Gleaves, G.S. Yablonskii, P. Phanawadee, Y. Schuurman, Appl. Catal. 160 (1997) 55.
[5] M. Rothaemel, M. Baerns, Ind. Eng. Chem. Res. 35 (1996) 1556.
[6] M. Soick, D. Wolf, M. Baerns, Chem. Eng. Sci. 55 (2000) 2875.
[7] K. Chen, A. Khodakov, J. Yang, A.T. Bell, E. Iglesia, J. Catal. 186 (1999) 325.
[8] D. Creaser, B. Anderson, Appl. Catal. A 141 (1996) 131.
[9] M.Yu. Sinev, V.S. Arutyunov, in: Proceedings of the 5th International Congress on Oxidation Catalysis, Sapporo, Japan, September 25–30, 2005, p. 164 (Program, Abstracts).
[10] M.Yu. Sinev, V.S. Arutyunov, A. Romanets, Adv. Chem. Eng. 32, doi:10.1016/S0065-2377(07)32003-6, in press.
[11] K.T. Nguyen, H.H. Kung, J. Catal. 122 (1990) 415.
[12] V.P. Vislovskiy, T.E. Suleimanov, M.Yu. Sinev, Yu.P. Tulenin, L.Ya. Margolis, V. Cortés Corberán, Catal. Today 61 (2000) 287.
[13] M.Yu. Sinev, J. Catal. 216 (2003) 468.
[14] J. Warnatz, Rate coefficients in the C/H/O system, in: W.C. Gardiner, Jr. (Ed.), Combustion Chemistry, Springer-Verlag, New York, 1984.
[15] W. Tsang, R.F. Hampson, J. Phys. Chem. Ref. Data 15 (1986) 1087.
[16] W. Tsang, J. Phys. Chem. Ref. Data 17 (1988) 887.
[17] R. Atkinson, D.L. Baulch, R.A. Cox, R.F. Hampson Jr., J.A. Kerr, M.J. Rossi, J. Troe, J. Phys. Chem. Ref. Data 26 (1997) 521.
[18] NIST Chemical Kinetics Database, v. 2Q98, 1998.
[19] M.Yu. Sinev, Catal. Today 13 (1992) 561.
[20] M.Yu. Sinev, Catal. Today 24 (1995) 389.
[21] M.Yu. Sinev, V.Yu. Bychkov, Kinetika i Kataliz (Russ. Kinet. Catal.) 34 (1993) 309.
[22] G. Veser, M. Ziauddin, L.D. Schmidt, Catal. Today 47 (1999) 219.
[23] D.I. Iordanoglou, A.S. Bodke, L.D. Schmidt, J. Catal. 187 (1999) 400.
[24] A. Beretta, P. Forzatti, E. Ranzi, J. Catal. 184 (1999) 469.
[25] A. Beretta, L. Piovesan, P. Forzatti, J. Catal. 184 (1999) 455.
[26] M. Fathi, R. Lødeng, E.S. Nilsen, B. Silberova, A. Holmen, Catal. Today 64 (2001) 113.
[27] O.V. Buyevskaya, M. Baerns, Catal. Today 42 (1998) 315.
[28] S.R. Morrison, The Chemical Physics of Surfaces, Plenum Press, New York, 1977.
[29] E.V. Kondratenko, S.A.R. Mulla, O.V.M. Buyevskaya, Baerns in 5th International Congress on Oxidation Catalysis, Sapporo, Japan, September 25–30, 2005, p. 342 (Program, Abstracts).
[30] E.V. Kondratenko, O.V. Buyevskaya, M. Baerns, Top. Catal. 15 (2001) 175.
[31] V.P. Vislovskiy, V.Yu. Bychkov, M.Yu. Sinev, N.T. Shamilov, P. Ruiz, Z. Schay, Catal. Today 61 (2000) 325.
[32] V.Yu. Bychkov, M.Yu. Sinev, V.P. Vislovskiy, Kinetika i Kataliz (Russ. Kinet. Catal.) 42 (2001) 632.